Smart Agricultural Technology 9 (2024) 100606

Contents lists available at ScienceDirect

Smart Agricultural Technology

journal homepage: www.journals.elsevier.com/smart-agricultural-technology

Autonomous collaborative mobile robot for greenhouses: Design, development, and validation tests

Fernando Cañadas-Aránega [a,*], José C. Moreno [a], José L. Blanco-Claraco [b], Antonio Giménez [b], Francisco Rodríguez [a], Julián Sánchez-Hermosilla [c]

[a] Department of Informatics, CIESOL, CeiA3. University of Almeria, 04120, Almeria, Spain
[b] Department of Engineering, CIESOL, CeiA3. University of Almeria, 04120, Almeria, Spain
[c] Department of Engineering, CIAIMBITAL, CeiA3. University of Almeria, 04120, Almeria, Spain

ARTICLE INFO

Keywords:
Mediterranean greenhouse
CoBot
3D design
ROS 2
SLAM
Sensors for navigation
Sensors for collaboration

ABSTRACT

This paper describes the development of a mobile agricultural robot capable of performing high-capacity transport tasks within greenhouses in presence of people or other agricultural machines. The main objective is to provide the robot with enough technology to work collaboratively with nearby human workers. In addition, the robot must also be able to transport 100 kilograms in a safe way over uneven terrain, a characteristic not usually found in existing greenhouse robots. This is important to ensure the sustainability of intensive greenhouse cultivation, as it is essential to allow more flexible use of robots when adapting. This would allow for expanding infrastructure size and operating volume to suit different greenhouse conditions, thus maximizing production. The robot is fitted with different sensors to enable autonomous navigation, perception, and to identify the environment and the operators (3D LiDAR, stereo cameras, and ultrasound). It also features the hardware necessary for cloud connection to share data in real time. All sensors have been validated to work correctly, hence the robot can move around the greenhouse. With the software currently used for collaborative robotics, the ultrasounds correctly identify the environment, and cameras and LiDAR can locate the farmer correctly. In this work, several gaps in greenhouse robotics are addressed by designing, developing, and validating a collaborative mobile robot with advanced sensors and algorithms with IoT integration. The robot lays the foundation for the implementation of autonomous navigation, collaborating with farmers in real-time and efficient operation in complex greenhouse environments, laying the groundwork for future advances in agricultural automation.

1. Introduction

In recent years, many researchers have focused on analyzing the importance of greenhouses, speculating on the results and significance of the state of the land and demand in the next 20 to 30 years [51,19]. The Food and Agriculture Organization of the United Nations (FAO) anticipates that by 2050, demand will increase by 70% due to overpopulation and the demand for food for humans and animals [24]. Based on these data, achieving efficient and sustainable agricultural production in an increasingly urbanized environment is essential, considering the decrease in arable land and increased labor costs [31]. In this scenario, plastic-intensive crop production has become the best alternative, which, following the COVID-19 pandemic, has highlighted the importance of safety in the agro-food sector [23]. Greenhouses cover an area of 496.800 hectares globally, with 42.7% of them located on the Mediterranean coast [34]. Although robotic harvesting has been successful in large-scale crops, limitations arise in other areas of agriculture. Factors such as the cost of investment and the need for specialized knowledge to maintain and operate the robots may hinder smallholder farmers' adoption of this technology. It is also essential to consider the potential impact on employment in the sector, as robotics could move human workers. However, despite these difficulties, agriculture is adopting more advanced technology that improves production, allowing a shift from small to large farms with less labor. The use of this technology is crucial, and currently automation and agricultural robotics techniques focused on machine-to-machine communication and, more importantly, machine-to-human interaction are being applied [11]. The development of robotic technologies for agriculture is expected to in-

* Corresponding author.
E-mail addresses: fernando.ca@ual.es (F. Cañadas-Aránega), jcmoreno@ual.es (J.C. Moreno), jlblanco@ual.es (J.L. Blanco-Claraco), agimfer@ual.es (A. Giménez), frodrig@ual.es (F. Rodríguez), jusanche@ual.es (J. Sánchez-Hermosilla).

https://doi.org/10.1016/j.atech.2024.100606
Received 30 July 2024; Received in revised form 11 October 2024; Accepted 11 October 2024
Available online 17 October 2024

crease considerably in the next 30 years, as it is an active area of research and innovation [38]. Despite existing challenges, such as customizing robotics for diverse climatic and topographical conditions, it is imminent as the world tends toward robotization, which, through human interaction, will combine strength and precision to develop efficiently operated greenhouses.

To make greenhouses the most viable solution, the adoption of technology must be an essential part of this process, particularly the automation and robotization of the various procedures involved in vegetable production. This encompasses the entire process from transplanting to transporting the product to destination markets, including the stages of harvesting and post-harvesting autonomously. However, the delicate nature of the environment poses challenges for robots in greenhouses, as they operate within a more complex system than robots in industrial or agricultural settings. These robots are affected not only by the characteristics of crops (such as color, size, shapes, textures, and variable locations) but also by environmental factors (such as lighting, positioning of fruits, branches, and leaves, monitoring of the health of the crop lifecycle and cutting of the soil) and, in addition, by elements and people in constant motion [55]. Moreover, for a mobile robot to navigate diverse environments and effectively accommodate crop variability, it is essential to implement localization techniques [6,39], which require exhaustive adaptation of sensors to this environment. Consequently, numerous research institutions are dedicated to improving the detection capabilities of the robot through technologies such as cameras, radio frequency identification (RFID), and magnetic systems, refining the robot's design for better adaptation to its surroundings, among others [46,62,65]. However, this task is complicated by the fact that, as is well known, navigation using elements such as a Global Navigation Satellite System (GNSS) or a Global Positioning System (GPS) does not work well indoors [48], especially within greenhouses, where crops are very close together and continue to grow [3]. This becomes one of the main problems of this type of application and, consequently, one of the main objectives of current research in greenhouses. This challenging task can be considerably improved by applying high-level techniques that use local sensors, comparing internal models to correct the trajectory [21], a concept currently known as a "digital twin". In order to maximize production, there is increasing emphasis on the use of cooperative techniques that allow robots to work with the environment. These techniques, for example, can help robot self-localization [26]. A powerful application is when these techniques are used to collaborate with humans or farmers, which means a close human-robot collaboration that aligns with "Collaborative Robotics". Equipping agricultural robots with sensors that allow them to observe and listen to the farmer and then act accordingly is a significant advance in robotics, considerably increasing the complexity of robot design [63]. Combining Internet connectivity allows robots to cooperate with other machines or elements installed in the greenhouse, further maximizing productivity [41]. In this case, components that offer wireless connection to a server must be added to connect the robot to the Internet of Things (IoT). In addition to managing the large amount of data collected by the sensors (Big Data management), it allows implementing "cooperative robotics" algorithms, one of the main objectives of the project funding this work [40].

Agriculture robots for planting, transplanting, pollinating, applying plant protection products, transporting materials, and harvesting tasks require specific technology to perform autonomous navigation in greenhouses [55]. However, only some prototypes have sensors and algorithms that allow one to establish collaboration between robots and humans. They have environmental perception sensors for navigation, ranging from LiDAR for mapping to RGB-D (red, green, blue, and depth) cameras that can detect and identify objects with their depth. With the help of laser technology, [1] presented a Robot Operating Systems (ROS) based navigation method with a 2D LiDAR on the "AgriEco" robot inside a raspberry greenhouse, carrying out the transport of objects. In [16], a similar work is presented in which Simultaneous Localization and Mapping (SLAM) is performed with a LiDAR and a RGB-D camera in a narrow greenhouse with a tomato crop to transport vegetable crates. Regarding related data, [15] presents a greenhouse model and a greenhouse mapping dataset with a novel SLAM technique with two LiDARs, whose data, from a tomato plantation, were recorded for two months. This information helps to optimize the application of plant protection products by coordinating the robot's speed and spray rate [57,56]. Although many works are related to robotics in greenhouses [58], few carry out collaborative control for robots. In [67], collaborative telerobotics techniques are applied inside a greenhouse to monitor the life cycle of plants in collaboration with farmers. Subsequently, in [66], different planning techniques used in greenhouses with robots are described to obtain higher agricultural yields, considering the flow of local farmers in the environment. In [20], different collaborative control techniques are applied in greenhouses on a differential mobile robot in simulation, in which objects emulating people are placed. In this case, it is observed how existing works perform mathematical applications or simulations in greenhouses, but none of them is applied in a real environment. To date, work with collaborative robots in greenhouses has been based only on simulated systems or basic tasks without implementing novel techniques. This work focuses on validating the design and sensors needed for collaborative work.

In this way, the main gaps observed in the literature according to the above review are the following ones:

- Collaborative robotics in real greenhouse environments: Although previous research has mainly focused on simulations or theoretical models, this paper fills this gap by developing and testing a collaborative mobile robot in a real greenhouse environment. This work addresses the challenge of human-robot interaction using cameras (a monocular one from Orbbec and a stereo one from Bumblebee) and currently employed algorithms (ORB_SLAM, MoveNet, and MOLA), allowing robots to work together with farmers in dynamic and complex environments such as Mediterranean greenhouses. To achieve this, mechanical design is a trivial step, placing each sensor in place to ensure its correct functioning. Each of these algorithms can identify the operator in its full range of vision, which is a fundamental step in ensuring the safety and integrity of the system. This practical application of collaborative robotics significantly advances previous work but needs real-world validation.
- Challenges of robotic navigation and adaptation to greenhouse conditions: Greenhouse environments present unique challenges for autonomous navigation, such as the inefficiency of GPS/GNSS systems and the need for robots to adapt to diverse conditions, such as dense crops, variable lighting, and complex topography. This paper addresses this shortcoming by thoroughly testing current algorithms used for navigation, such as vision-based systems and SLAM algorithms with cameras (two cameras, Orbbec and Bumblebee) and LiDAR (Velodyne VLP16), and validating them in a real greenhouse, placing them under rigorous mechanical design in locations where maximum efficiency is obtained. This helps solve the critical problem of indoor navigation and adapts robotics to the specific environmental requirements of greenhouses.
- IoT integration and Big Data management to improve agricultural efficiency: The paper addresses the gap related to IoT integration and data-driven agriculture by equipping the robot with the ability to connect to IoT systems. The onboard PC has a wireless connection card with 802.11ax connections, which, together with long-range antennas, can pick up WIFI waves to 10 meters. This will enable real-time monitoring, data management, and interaction with other machines, increasing the potential for more efficient and automated greenhouse operations. IoT integration is essential in agriculture, where machines can operate collaboratively and autonomously, maximizing productivity due to real-time data exchange and improved decision-making.

- Real-world testing and validation of robotic systems: Many studies on greenhouse robotics have remained theoretical or based on simulations. This paper fills this gap by validating the robot design and navigation systems through real-world testing with farmers. For this purpose, the robot was taken to the IFAPA greenhouse at the AGROCONNECT facility, where it was fully completed and tested. All sensor locations were validated with the farmer, and the different algorithms were used. This practical approach ensures the technology is feasible and effective in real agricultural environments, providing a fundamental basis for future developments and improvements.

In general, this work contributes extensively by addressing critical gaps in greenhouse robotics, from the development of collaborative robots in real-world environments to the approach to solving technical challenges related to navigation, IoT integration, and adaptation for various farming environments. It lays the foundation for future innovations in autonomous and collaborative farming, especially in complex environments such as Mediterranean greenhouses, and establishes a solid basis for real-world testing and further technological development.

The rest of the document is organized as follows: Section 2 describes the specifications that have been taken into account for the design of the collaborative robot. Section 3 comment the design stage of the robot, focusing on the electronic, electrical, and mechanical aspects. Section 4 discusses the actual test sites where the tests were performed. Section 5 shows the validated results of both the real robot and the sensors from a collaborative robotics point of view. Finally, section 6 presents the conclusions and future work.

2. Design specifications

In this section, the specifications and security restrictions from the current standards for the robot design are described. In order to achieve a collaborative agricultural robot able to cooperate with other robots in a greenhouse, the main objectives and the standards to be followed for the design are:

- Construction of a medium-sized platform with a high degree of maneuverability. To achieve this, the design must comply with the main safety standards for agricultural robotics, particularly emphasizing the principles of highly automated machine design (ISO 18497:2018) and their control (ISO 11783:2001). Furthermore, it is necessary to consider the technical guide from the National Institute for Safety and Hygiene at Work (INSHT) on manual handling of loads, which defines the most important guidelines that any operator must consider for weight manipulation. More specifically, the robot must adhere to the basic non-industrial robot standards (ISO 13482:2014), with a focus on mobile robotics application (ISO 23482-2:2019), as well as safety requirements for industrial mobile robots (ANSI/RIA R15.05-1:2020).
- Considering all the safety standards mentioned in the previous paragraph, one of the most critical requirements revolves around the robot's speed. It must be able to move at approximately 0.5 m/s (ISO 18497:2018), thereby ensuring both its own integrity and the safety of the surrounding environment.
- The transporting is the main task to be performed by the robot, assisting the farmers while they are harvesting. It must be capable of carrying a maximum payload of 100 kg through the greenhouse, ensuring stability even at maximum weight, as indicated in the ISO 18497:2018 standard.
- The robot must be able to navigate in outdoor, so that it is able to move for example between different greenhouses.
- It must be able to navigate autonomously within a typical plastic Mediterranean greenhouse, which accounts for 92% of the total greenhouse area worldwide (estimated at around 500,000 ha [53,34]). To this end, it must be equipped with sensors oriented towards the recognition of objects, other robots, and farmers working alongside it, validating the correct functioning of each sensor with the most common algorithms currently in use.
- It mus be able to work in a collaborative way with the farmer and in a cooperative way with other robots.
- The robot must be able to connect to the cloud.
- It should be an energetically efficient robot, considering the possibility of meeting its energy needs with renewable sources. This is essential to ensure sustainability in greenhouse interior transportation.

2.1. Mechanic design specifications

The robot must be able to transport as many crates as possible throughout the greenhouse to save as many trips as possible between the point of origin and the destination. This poses a new challenge: to facilitate efficient transport by the operator and to achieve a balance between size and maneuverability in the middle of the crops while saving as much energy as possible.

On the one hand, from a design point of view, the ISO 13698-1:2003 and ISO 5687:2018 standards, which define the European pallet at 1200 × 800 mm for the storage of fruits and vegetables, used by local farmers in the region, aligning their infrastructure and daily operations with this standard, ensure a uniform national transport system. Furthermore, by European Regulation No. 543/2011, which standardizes and advises on the preservation of various vegetables, the dimensions of a box of aubergine, zucchini, and cucumber are defined as 0.50×0.37× 0.26 m, while peppers have dimensions of 0.60×0.40×0.32 m. The platform base must be able to carry at least two boxes of peppers, representing the most unfavorable scenario in terms of size.

On the other hand, from the point of view of operator ergonomics, the European Agency for Safety and Health at Work (EU-OSHA) and European Union Directive 90/270/EEC and ISO 1503:2008 advise that an operator performing manual weight handling work should not deposit heavy weight below his hip, causing the robot to be designed with a height of 0.5 - 0.7 m to ensure safe manual transportation [22]. Similarly, to align with the dimensions of the Mediterranean greenhouse, where plants are placed in corridors with a width of 0.90 m to 1.10 m, the maximum width of the robot is 0.6 m, adhering to the standard dimensions of a box of peppers. The resulting chassis must be adjusted to the dimensions of the greenhouse, taking into account the width of the aisles and the space required to change the corridors. Finally, considering that the transported boxes occupy a space of 0.8 m, and taking into account the sensors, it was decided that the robot should be 1 m long. In addition, this measurement allows the robot to rotate between corridors inside the greenhouse.

2.2. Sensors design specifications

In this section, an analysis of the specifications for the sensor subsystem will be performed, determining the placement of each element on the robot. It is important to note that this section details the physical location for each robot's component. To see the interaction at the software level, go to the section 5.2, where the algorithms used for each sensor and their interactions are detailed. More specifically refers to Fig. 22, special emphasis is placed on local robot communication.

In this case, ISO 26262-5:2018 determines the security conditions established from the hardware point of view.

An optical system capable of identifying objects and people in its surroundings must be installed to ensure optimal navigation for collaborative robotics. Based on local farmers' experience, objects that a robot can encounter in this agricultural environment typically have a size ranging from 20 to 120 cm in height, a factor that must be considered when designing the robot. Since image local interpretation involves a high computational cost, it is advisable to install an embedded system connected to the main computer to process the captured images of people, decoupling the recognition of the operator's pose from the navigation. In the latter case, the optimal height to identify the average stature of a person (1.8 m, as cited in [61]) is calculated to be 1.65 m away. This is another crucial aspect to consider in vehicle design.

One of the most common sensors used for navigation is the LiDAR sensor. This element performs a 360 degree mapping of the environment, generating a 3D map for navigation and identifying items and people. These components typically have a vertical measurement range, which requires the sensor to be placed in a location accessible from obstacles throughout the horizontal plane to maximize its field of vision. To ensure safe autonomous navigation, the installation of ultrasonic sensors is very important [44], achieving fault-tolerant redundancy that helps other sensors. This type of device uses high-frequency sound waves (ultrasonics) to detect the presence or distance of objects in their surroundings. These sensors must be installed around the robot's perimeter.

Finally, wheel speed sensors are one of the most essential components of the robot. It is responsible for providing real-time information about the robot's speed. Typically, you are expected to find them installed together with the motors in the same package, although at times it may be necessary to install them near the drive shaft.

2.3. Actuators design specifications

Initially, the different configurations and typical actuators used in today's literature are analyzed. The use of electric motors reduces the noise level and CO^2 emissions in an enclosed environment such as the greenhouse, making the work of the operators inside the greenhouse safer. In addition, it would allow the implementation of photovoltaic recharging systems, increasing the sustainability of greenhouse operations [64]. However, in the experience of the authors in this field, the use of a *Ackerman* steering system reduces damage to the soil, especially during turns, compared to a differential steering system. In this respect, it has to be considered that most greenhouse floors are loose soils and that the vehicles used in the operations have to turn into very tight spaces. In this case, two motors are required: one will be responsible for traction, while the other will be responsible for steering the robot.

In this case, ISO 23482-2:2019 clarifies and provides guidance on new safety terms and requirements introduced to enable close human-robot interaction and human-robot contact in personal care robot applications, including mobile servant robots, physical assistant robots, and human-carrying robots. In the case of actuators, the interaction with the host computer will be explained in the section 5.1 as only physical considerations have been considered.

2.4. User interface design specifications

Another important aspect that requires specification is the user interface. In this case, mobile robots must comply with a series of regulations that, on the one hand, meet basic safety standards and, on the other hand, enable the machine to interact easily with the operator. This interface comprises software programming that will allow easy human-machine interaction and the programmer to access machine control. In addition to this characteristic, it is also important to ensure accessibility to safety hardware, which requires a control panel to ensure the integrity of the robot and the environment [4].

On the one hand, the ISO 15066:2016 standard determines the necessity of implementing a device that emits a warning signal when the robot works in a collaborative environment with humans. In this case, the signal shall be both acoustic and visual, ensuring human-machine collaboration. This device will preferably be installed in the farmer's field of vision, displaying the necessary amount of information to guarantee the total integrity of the robot and the operator.

On the other hand, the ISO 13482:2014 standard obliges the designer to implement various manual physical mechanisms that determine safety during the robot's tasks. In this case, the robot must be connected manually, never automatically, to avoid unwanted behavior. A manual control mechanism must be installed to allow the operator to control the robot's direction and speed. In addition, a safety button should be placed in the most accessible area possible so that the operator can stop the machine in an emergency.

3. Mechatronic design of the robot

This section describes the mechanical and electronic components chosen for the subsequent design of the robot. Typically, a robot's design follows a recursive approach to mechanical design by covering the actuator, sensor, and control subsystems. However, it has chosen to describe the actuators, sensors, and controller first and then the mechanical design to better understand the final prototype.

3.1. Electronic components

In the case of sensors, the robot will be fitted with the latest technology to self-locate, perceive the environment, and guarantee the safety of the operators when the robot is working next to them. It has been chosen:

- *Stereo camera Bumblebee BB2-08S2*[1]: It has two lenses for capturing synchronized stereo images. It connects to the PC through a FireWire IEEE 1394 interface, providing a data transmission speed of 800 Mb/s. The stored data has a resolution of 1032 x 776 pixels. The field of view is 97° horizontally and 66° vertically within a range of 0.3 m to 20 m. Recording is done at 10 Hz, with a maximum frame rate of 20 fps and with a consumption of 1 A at 5 V. The camera is situated at the front to capture images suitable for identifying people and items or for guiding a robot through the corridors of the greenhouse.
- *Orbbec Persee +*[2]: The 3D camera possesses a sensing range from 0.6 to 8.0 m and functions effectively within temperatures ranging from 0° to 50°. This camera contains an embedded Linux or Android operating system on an Arch 64 processor capable of running complex systems inside. The Persee + model also provides connectivity options, including High Definition Multimedia Interface (HDMI), Bluetooth 5.0, and RJ45 Gigabit Ethernet with a consumption of 1.8 A at 5 V. This camera is intended to identify the pose of people as the robot works next to them, with the possibility of elaborating different collaboration strategies with humans in the future.
- *Ultrasonic kit Valeo*[3]: This kit contains twelve ultrasonic sensors, one Engine Control Unit (ECU), sensor holders, and one harness. The operating range is between 0.15 and 4.00 m, with a horizontal angle of 75° and 45° vertically via Controller Area Network (CAN) protocol. They operate between 11 and 16 V with a power consumption of 6 W. This sensor is intended to detect objects close to the robot's perimeter.
- *NOVATEL SPAN-IGM-A1*[4]: This GNSS offers a inertial navigation tightly coupled with an OEM615 receiver. It has a level accuracy of one meter to one centimeter, with operation between 10-30 $V\,DC$ regulated with a power consumption of 0.87 A. It can be connected via serial, USB, CAN, and Multi I/O interface and is compatible with GPS, Globalnaya Navigatsionnaya Sputnikovaya Sistema (GNSS), Satellite Based Augmentation System (SBAS), and Real-Time Kinematic (RTK). In this case, this device will be used to obtain the positioning when the robot performs tasks outside the greenhouse between warehouses.

[1] Bumblebee BB2-08S2 (website).
[2] Orbbec Persee + (website).
[3] Ultrasonic kit Valeo (website).
[4] NOVATEL SPAN-IGM-A1 (website).

- *ANTCOM 42G1215X ARINC Antenna*[5]: This dual-band L1/L2 GPS antenna is connected to the Novatel SPAN-IGM-A1, with a power consumption of 1 W. The active configurations offer 2-stage integrated bandpass filtering for high out-of-band rejection and limiter diodes to protect sensitive receiver electronics. Thanks to its high-frequency range, it can provide the triangulated position with nine satellites with an error of 50 cm. In this case, the antenna requires installation because it is expected that the robot will have to perform areas outside the greenhouse, which, being in the open, provides a correct location.
- *HISTTON PC*: Greenhouses frequently experience harsh environmental conditions characterized by high temperatures and humidity levels [33]. In light of these challenges, the platform is outfitted with a HISTTON computer featuring an Intel i7-8550U processor (4 GHz), an Intel UHD 620 graphics card with 24 Computers Unified Devices Architecture (CUDA) cores, and 32 GB of memory DDR4 Random Access Memory (RAM). This selection was made based on its ability to operate within a temperature range of 0 to 70° and a humidity range of 0 to 85%. Consuming a mere 15 W, it demands minimal power, which is crucial to consider for battery capacity. Furthermore, the computer is configured with two disk partitions to accommodate both Ubuntu 20.04 with ROS Noetic and Ubuntu 22.04 with ROS 2 Humble, allowing users the flexibility to work with either version. It is important to note that this computer is equipped with a Wireless Fidelity (WIFI) network card whose wireless connection protocol is IEEE 802.11 ac (connections up to 1300 $Mbps$). This is ideal for establishing the pillars of cooperative robotics.
- *Elecrow 10.1'*[6]: It is important that the robot has a device that is able to display the main characteristics of the sensors. For this design, the 10.1' Elecrow touch screen will be installed, which operates at 12 V and has a power consumption of 0.9 A. It has a HDMI connection. In addition, it has two 15 W loudspeakers that can emit sounds to alert the environment, which makes it a device that adapts to the specifications of the previous section.
- *Controller I24-70*[7]: For manual control, a mechanism that allows the robot to move forward or backward with a turn is added. To provide it with motion, a PG Drivers SK76977 (model I24 - 70) controller is installed, which changes the setpoint to the speed through a potentiometer and a joystick to set the advance or retardation. This reprogrammable DC controller can work with currents of up to 70 A. It has a battery and motor pin that can be controlled using a manual potentiometer. In this case, the manual operation mode will be determined as this article does not focus on the robot's control. On the other hand, the steering control is done by a second joystick, which drives the front motor in one direction or the other. In this case, the control is carried out by commutation thanks to two Schneider limit switches, which set the physical limits of rotation.

Finally, sensors have been installed to identify the pulse for future navigation. These elements are described in the following:

- *Encoder SICK DBS50E*[8]: This lap meter has a resolution of 1000 pulses per revolution, which provides high resolution. It is powered between 3.3 and 30 V, operates at up to 8000 rpm, and, in addition, has a zero-crossing sensor "Z" to mark one origin per turn. For the PC to be able to read the encoder, a Phidgets 1047 data acquisition card[9] is installed, with a capacity of up to 4 encoders with reading of channels A, B and index.

[5] ANTCOM 42G1215X (website).
[6] Elecrow 10.1' (website).
[7] Controller I24-70 (website).
[8] SICK DBS50E (website).
[9] Phidgets 1047 (website).

- *Limit switch ZCP21*[10]: This identifier can cut off currents of around 10 A at 220 VAC at an activation speed of 0.01 m/s. This is installed to determine the maximum turning limit mentioned above.

In Fig. 1, one can see the schematic of the sensors with their physical means of connection.

3.2. Actuation and power components

In this section, the actuators and the power element shall be studied and selected, considering the considerations in Section 2.

- Motors

The robot must be able to move a 100 kg payload. In addition, the weight of the robot's mass for movement must be added. Taking into account the density of the S275J steel (material to be used for the construction), the estimated weight of the structure with all components will be 291 kg (data obtained from the 3D design of Section 3.4). If a safety factor of 1.5 [37] is used, a final value of 378.3 kg is obtained. Considering that a speed of 0.5 m/s is required, it is possible to determine the power needed to move it. To carry out this calculation, the method developed in [32] has been followed through the Eq. (1) and (2) since it takes into account the mass itself, and the friction of the wheels on the ground as shown in the Fig. 2.

$$F_{Pull} = F_{Weight} + F_{Friction}, \tag{1}$$

$$F_{Pull} = mg\sin(\alpha) + \ \mu mg\cos(\alpha), \tag{2}$$

where F_{Pull} is the force required to move a mass, F_{Weight} is the force of the robot's own weight (supposed with mass m), taking into account the friction force $F_{friction}$ on sandy soil (where μ is the rolling resistance coefficient with the ground, with a value of 0.5 according to [35]), F_N corresponding with the perpendicular component of the weight applied on the ramp, and with a slope of angle α to the horizontal (between 1% and 2% due to the typical characteristics of a Mediterranean type greenhouse). The power needed to drive the robot responds to the Eq. (3).

$$P_{max_T} = F_{pull} \cdot v_{max}, \tag{3}$$

where v_{max} is the maximum speed, equal to 0.5 m/s as was previously commented. In this case, the traction motor must have a power greater than 463.84 W, so a 500 W and 24 V ECM350/030[11] motor is chosen. This motor is ideal for use in greenhouses. It has IP66 protection, so it will not be damaged by humidity and dust, and an H23 stop brake, which increases its safety for working with humans. It will stop if it suffers a power cut.

On the other hand, the steering motor requires the pivoting momentum between the ground and the wheels, commonly called "Torque" or "$M_{steering}$." In this case, the method followed in [27] has been used in Eq. (5), which takes into account the friction of the tire with the ground, as shown in Eq. (4).

$$M_{steering} = F_{weight} \cdot \rho_p, \tag{4}$$

$$P_{max_S} = M_{steering} \cdot \omega_{max}, \tag{5}$$

where ρ_p is the friction coefficient of wheels and ω_{max} is the maximum angular velocity measured through the encoder. In this case, a power of 73.18 W is required so, that a CM100/040[12] motor of 140 W and 24 V is chosen. In this case, this motor is also ideal for use in greenhouses. As was previously commented, it has IP66 protection and an H23 stop brake.

[10] ZCP21 (website).
[11] ECM350/030 (website).
[12] CM100/040 (website).

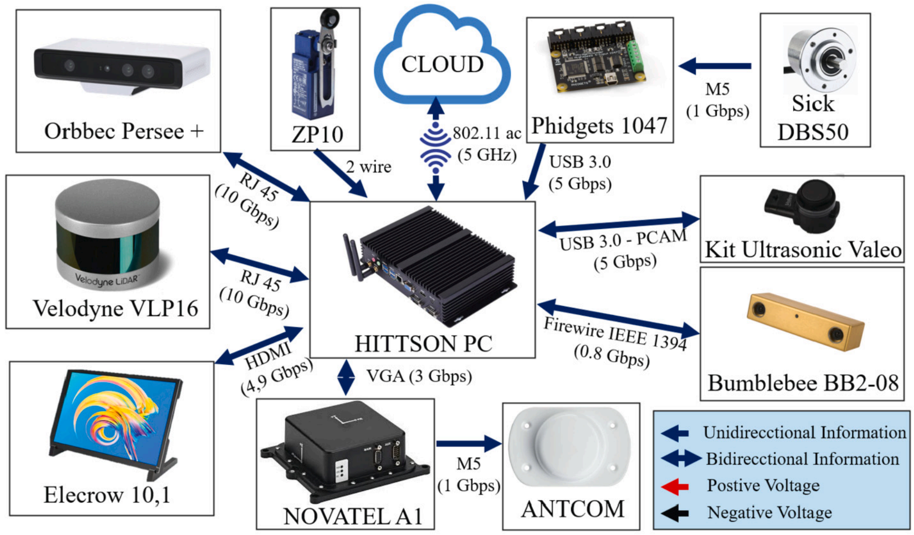

Fig. 1. Connection diagram of the electronic components.

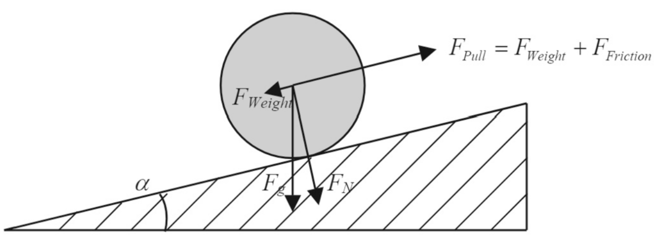

Fig. 2. Simple vehicle model [32].

- Bearing

Once the power generated by the motor has been determined, the next step is to carefully select the bearings. Of all the bearings in the robot, the most critical is the one in the plane parallel to the ground, which carries all the weight. A double-row angular contact needle roller bearing, capable of supporting high axial forces (more compact axial profile), is usually used for this type of application. However, it risks breaking when the bearing cannot handle the axial load. To solve this problem, two similar bearings were used for all four wheels, replacing them with a double-row angular contact ball bearing. The capacities of this bearing are significantly high, although it was chosen mainly because of the space restrictions imposed by the inner diameter.

In this case, the bearing chosen is the model 51412 M from the SFK catalogue [59]. This bearing has a working load of up to 7.7 kN, supporting twice the weight for which the robot is designed. Moreover, as it is a pure axial load bearing, the robot gains stability on sandy ground, which, together with its robustness, allows it to withstand the irregular and sandy soil typical of greenhouses. In addition, this bearing requires lubrication with high-viscosity lubricants, which results in a maintenance requirement of once every six months. Finally, it is equipped with seals to retain the grease necessary for smooth rotational movement. Its service life is also remarkably long and can be calculated using specific formulae in [52], assuming that the bearing operates statically.

- Wheels

The robot will move mainly inside the greenhouse, and the ground in Mediterranean greenhouses is typically sandy and uneven. Therefore, wheels that can move without displacing soil, turn with minimal soil disturbance, and maintain vehicle stability will be selected. In this case, as the width of the corridor through which the robot must travel is 2 m and the objective is to maximize the support section between the wheels and the floor, a model with a diameter of 20 cm and a rolling width of 30 cm is chosen, guaranteeing a correct distribution of the weight. The tire is chosen from a local company, whose main characteristics are centered on the weight it can withstand, which is 120 kg per wheel (480 kg in total).

- Batteries

Once the power consumed by the motors and sensors is known, the next step is the selection of the batteries, which play a crucial role in a robot because the more significant the capacity, the greater the autonomy. The motors chosen will operate at 24 V DC, which determines the voltage at which the batteries must operate. The reference value takes into account the current consumed by the set of actuators and sensors, which is 26.6 A for the motors and 8.1 A for the sensors. Another critical aspect determining the battery's choice is the desired autonomy, as the robot must be capable of enduring an entire workday of harvesting use. Considering that a farmer works for 8 hours during the harvest season, the robot should not require charging during that period, and it does not constantly operate at maximum power. An autonomy of at least 4 hours is considered [18]. It is possible to determine the correct battery capacity using Ohm's Law from Eq. (6).

$$I = \frac{P}{V}, \tag{6}$$

where V is voltage in Volts, P is the power consumed, and I is current in amps. Shows the total current required to determine the autonomy for the propulsion and steering motor in Eq. (7).

$$I = I_T + I_S. \tag{7}$$

Obtaining a result of 26.67 A when the robot advances at maximum speed. Considering the consumption of sensors and considering that an autonomy of 4 hours, a battery of at least 136.8 Ah will be required. The NBA 4TG 12 NH,[13] capable of providing up to 157 Ah at 12 V voltage, was the battery chosen. Measurement of 345x170x285 cm in dimensions and weighting 37 kg. Therefore, two batteries will be installed in series, obtaining the necessary voltage for the motors and, using a 24-12 V converter RSD-100D-12,[14] for the voltage for the sensors.

[13] NBA 4TG12NH: (website).
[14] RSD-100D-12 (website).

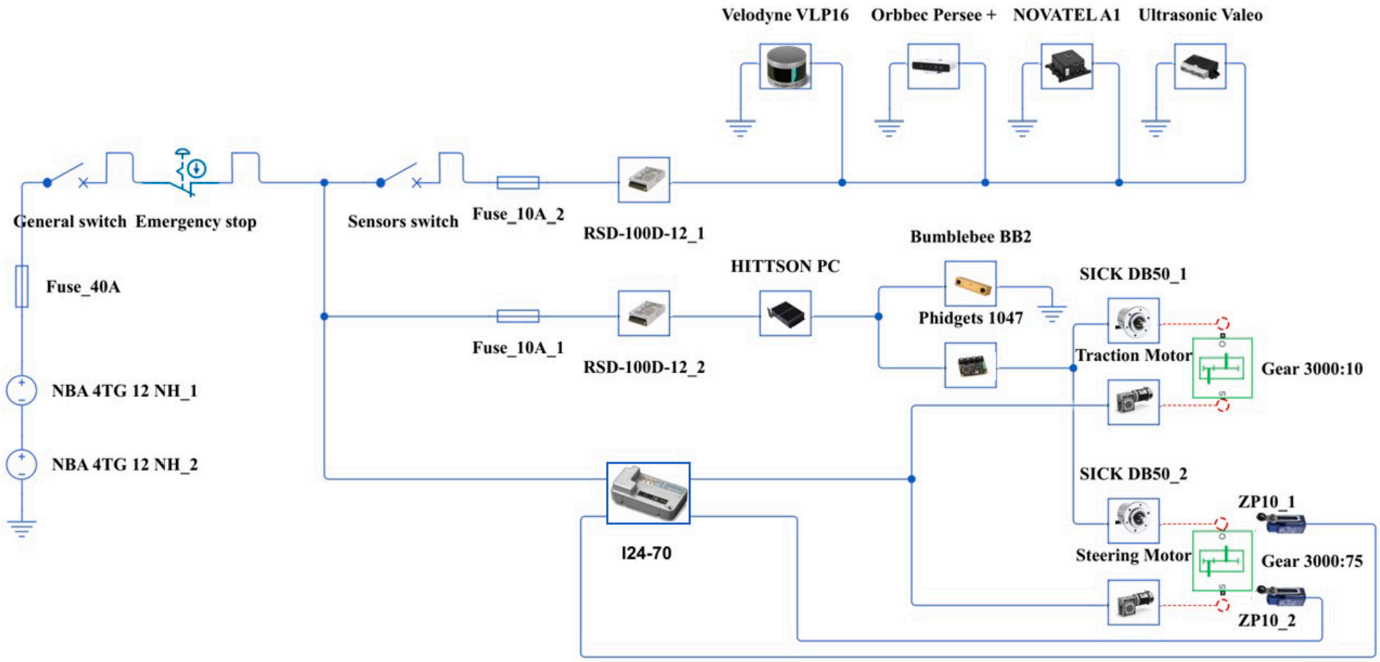

Fig. 3. Electric connection diagram.

In order to reduce human workload, the WIBOTIC [15] wireless charging station has been installed to allow the robot to charge autonomously when needed. In this case, the robot is fitted with the RC-100-WP receiver which, together with the OC-262-WP on-board charger, allows a 300 W inductive charging flow, achieving a full charge in a total of 13 hours. Fig. 3 shows an electrical diagram of the operation of all sensors, as well as their connection to the power supply.

3.3. Mechanical design

Once sensors, actuators, and power supply have been chosen, and without losing sight of the general considerations, the next step is to make the 3D model for the robot, from which the plans for its construction will be extracted. For the design, the CAE software SolidWorks Simulation® has been selected. SolidWorks is the leading CAD software for mechanical design, boasting a user-friendly graphical interface [60].

One of the most important aspects to take into account before starting the robot design is the weight and dimensions of the batteries (37 kg and 345x170x285 cm, respectively). They will be placed in the center of the robot and as close to the ground as possible, achieving a lower center of gravity and even weight distribution on all four wheels. The compartments will be prepared to house all electronics, characterizing the rest of the components with a rectangular profile of X40 [2]. Fig. 4 shows a view of the complete result.

The method of transmitting the movement of the motors to the different axles will be by chains, given their robustness [54]. In the case of the rear transmission, as can be seen in Fig. 5, two straight pinions are installed, seeking a transmission ratio between the traction motor and the ground so that the robot reaches a maximum of 0.5 m/s, as specified in the general specifications. Therefore, the driving pinion will have twenty teeth and the driven pinion forty, obtaining a transmission ratio of 0.000675, taking into account the reduction of the worm gear-crown of the motor itself.

In the case of the front transmission, no reduction gear will be installed, as it is considered that the rotational speed itself is sufficient to navigate the greenhouse. In Fig. 6, a 20-tooth sprocket is installed to change the transmission plane and is connected to both forks using a chain.

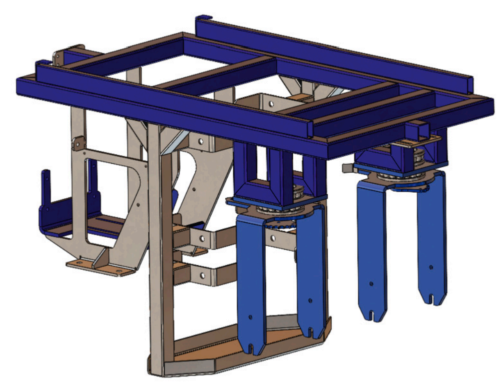

Fig. 4. Robotic chassis.

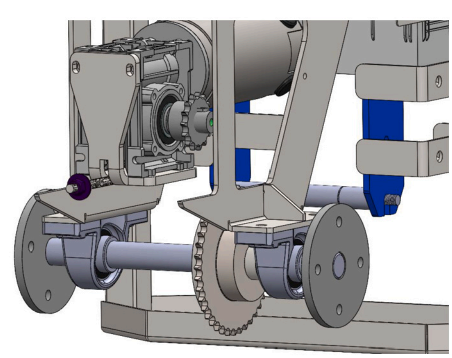

Fig. 5. Rear transmissions.

To ensure that ultrasonics can detect the environment, a front and rear bumper shall be designed to allow the robot to have a full view, achieved by a 45° chamfer horizontally. Based on this design, the dead spots of the robot should be adjusted to allow it to stop when approaching within 20 cm of the robot direction, according to ISO 18497:2018 and as shown in Fig. 7.

[15] WIBOTIC: (website).

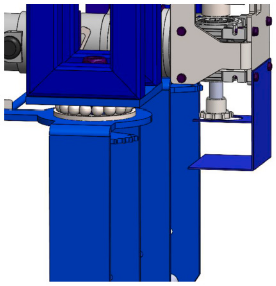

Fig. 6. Front transmissions.

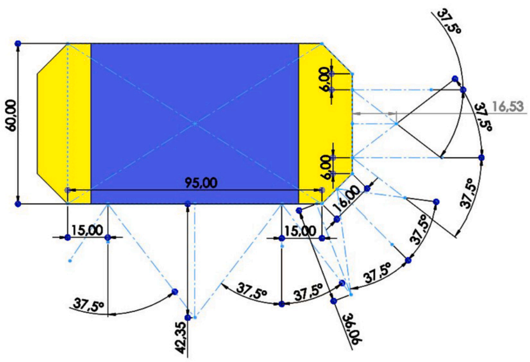

Fig. 7. Robot dead spots (dimensions in centimeters (cm)).

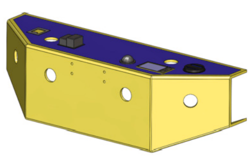

Fig. 8. Bumper.

The manual control panel will be placed on the rear bumper as, according to the ISO 18497:2018 standard, the robot must be manually connected, eliminating the possibility of remote activation. Installing an emergency stop button is mandatory to allow manual shutdown when the user needs it. Fig. 8 shows the result of this design.

Transport module is proposed for use inside the greenhouse. This is designed without sharp or potentially harmful terminal components that could injure the operator. Additionally, it provides an ample transport area capable of accommodating two standardized local vegetable crates. The design result is presented in Fig. 9a. The joining mechanism can be observed in Fig. 9b. Thanks to a rectangular X60 profile, it can slide and be replaced by another module, enhancing the robot's versatility and the potential for designing various agricultural implements.

Lastly, considering that some components must be positioned above the robot's base, it is necessary to design an element that remains fixed to the chassis and meets the desired height. In this case, a mast is chosen to be installed at an altitude of 1,5 m, allowing the placement of the camera for human identification, LiDAR, and GPS (see Fig. 10). This multilevel mast gives the robot additional capabilities and the possibility to study the interpretation of various sensors at different heights, estimating the most optimal one. Two X30 telescopic profiles are used. At the top, two platforms are installed: the first houses the LiDAR, and the second houses the GPS to capture most of the sky. Since the LiDAR requires 360-degree vision, the identification camera will also be installed on the upper platform. Finally, two plates are installed where the screens will be, one at the rear, where the supervision interface will be established, and the other at the front, where the interaction interface with the farmer will be designed, facilitating the collaboration between the machine and the operator.

3.4. Assembling of 3D model

To achieve this design, 491 components have been assembled, including screws, components, axes, and the main structure. The resulting 3D model of the robot is shown in Fig. 11.

The *Ackermann* configuration is distinguished by two front forks that define the robot's direction. In addition, side projection covers are installed, where the logos of the spindle protector will be placed. In the interior, all control units are placed. An exploded view of the resulting assembly is shown in Fig. 12, the description and location of which can be found in the Table 1.

All parts were connected with bolt patterns, the sheets were made by the operation corresponding to 3 mm thick metal sheets, and the elements were simulated to be spot welded. The result of the assembly was a success as it met all the requirements and exceeded the expectations. The stability result meets the minimum requirements, so the design results indicate that the prototype can be realized. Finally, the most important physical properties (density, elastic modulus, etc.) are shown in the Table 2.

4. Test facilities

The experiments were carried out at the Agroconnect facilities in the Municipal District of La Cañada de San Urbano, Almería. These facilities received co-funding from the Ministry of Science, Innovation and Universities in collaboration with the European Regional Development Fund (FEDER) as part of the grant program to acquire cutting-edge scientific and technological equipment in 2019. The location is at coordinates 36°50' N and 2°24' W, with an elevation of 3 m above sea level and a terrain slope of 1% in the North direction (refer to Fig. 13).

This kind of greenhose is characterized by a plastic cover and no climatic actuators such as heating, used only in critical events. They are multi-span greenhouses with a structure made of wood or galvanized steel. The average surface is around 1 ha, with spans of different sizes from 4 to 9 m, and even more, maximum height ranges from low greenhouses of just over 3 to 6-8 m. A central corridor, 2 m wide, serves as the main thoroughfare, branching into eleven aisles on each side. The North-side aisles measure 2 m wide and 12.5 m long, while those on the South side span 2 m wide and 22.5 m long. Radiating from the central aisle are narrower secondary corridor, each just one meter wide, facilitating the movement of mobile robotic units. The diverse array of robotic units operating within these facilities, including the mobile robots from the AGRICOBIOT[16] and AGRICOBIOT II[17] projects and maintenance drones, seamlessly integrates into this overarching architecture. These units operate with their fog-based systems, enabling them to access and contribute valuable information to and from the broader spectrum of systems in operation.

The crop usually grows in soil culture; it is the majority compared to soilless crops such as hydroponics. The most common form of cultivation is a soil modification called "sanding", which consists of placing different layers of soil on top of the original soil, which tends to be very clayey, or in other words, impermeable. The three layers usually used are: a layer of sand in the lower zone on top of the original soil, then a layer of manure, and finally a sandy layer that helps water droplets penetrate quickly and homogeneously to reduce evapotranspiration. Plants are placed in corridors with a width of 0.9 m to 1.10 m with two aims: to promote natural ventilation and facilitate labor for workers and machines. Greenhouses are used mainly for the production of vegetables, followed by ornamental plants. The main products are tomatoes, peppers, melons, watermelons, zucchini, eggplants, and strawberries.

It usually does not increase further due the effects of strong winds. The main actuator is the natural ventilation used to reduce the temper-

[16] Project identifier: UAL2020-TEP-A1991 (UAL/CTEICU/FEDER).

[17] Project identifier: PY20_00767 (CTEICU/FEDER).

(a) (b)

Fig. 9. Transport module.

Table 1
Description of the elements.

Element	Description	Element	Description	Element	Description
1	Porticoes	10	ECM350/030	19	Left fork
2	Display board 1	11	Protection plate right	20	Left bearing
3	Moving part of the mast	12	Rear right wheel	21	ECM100/040
4	Load support table	13	Front right wheel	22	Front bumper
5	Transport element	14	Right bushing	23	Front left wheel
6	ON/OFF button	15	Driving axle	24	Right bushing
7	Fixed part of mast	16	Right bearing	25	Right protection plate
8	Emergency shutdown	17	NBA 4TG 12 NH	26	Rear right wheel
9	Rear bumper	18	Right fork	27	Chassis

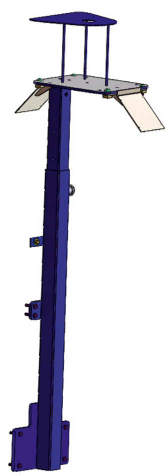

Fig. 10. Masthead.

Table 2
Physical properties.

Mass	291.38 [Kg]
Volume	1.22 [m^3]
Area of surface	0.953 [m^2]
Center of mass	(-0.112, -0.259, -0.023) [m^2]

ature and the humidity content. Oriented in an East-West ridge configuration, the design maximizes natural ventilation from the prevailing winds in the region. To ensure comprehensive monitoring of critical variables within the system and capture real-time meteorological conditions, both inside and outside the greenhouse, six interior IoT (Internet of Things, integrated into a larger cloud-based framework [50]) stations have been strategically positioned. These stations can measure various parameters, including temperature, relative humidity, ambient pressure, leaf humidity, solar radiation, PAR radiation, and CO2 concentration. Additionally, they can offer information on soil-related metrics such as volumetric content, electrical conductivity, and soil temperature. Furthermore, the infrastructure incorporates two external meteorological stations that track external variables such as precipitation, wind speed and direction, radiation levels, temperature, humidity and CO2 concentration [47].

Fig. 11. 3D model robot.

5. Robot operation validation

This section shows the validation results of the robot operation, verifying that the specifications in Section 2 have been met. Once the 3D model was completed, the initial prototype was built, it was reprofiled and machined again to refine all the crucial aspects, thus completing the prototype of the AGRICOBIOT II robot (see Fig. 14).

As can be seen, the real design complies with the specifications designed in the 3D model. The sensors comply with all the restrictions imposed in the design, resulting in a safe and robust robot that complies with all the regulations mentioned in Section 2.

5.1. Actuation subsystem validation

The motors must then be validated for the correct operation by verifying that the manual control system works correctly. For this purpose, two tests were performed inside the greenhouse, a speed test of the traction motor and a steering test of the steering motor. From these tests,

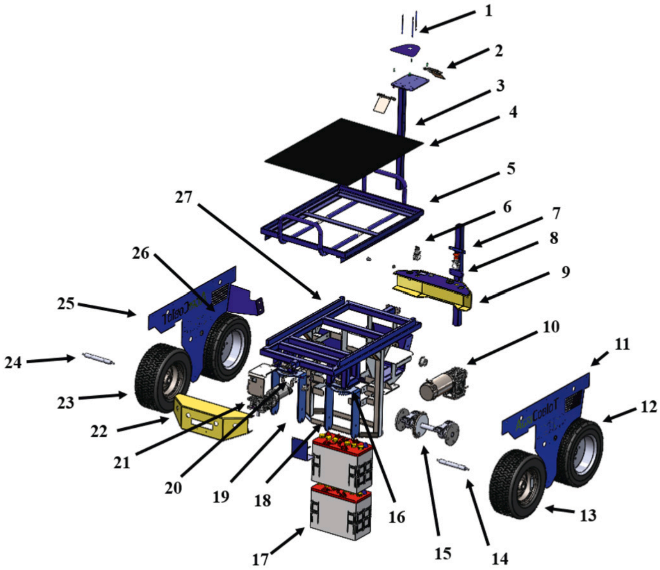

Fig. 12. 3D robot model - exploded view.

(a) Greenhouse outdoor

(b) Greenhouse indoor

Fig. 13. Agroconnect greenhouse.

Fig. 14. AGRICOBIOT II Robot.

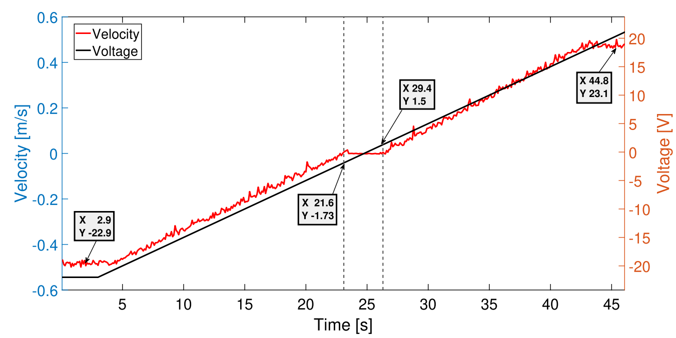

Fig. 15. Dead-Zone response and limited saturation response of traction motor.

the dynamic operating behavior and the dead-zone of the engines were obtained.

5.1.1. Traction motor

The I24-70 controller has different pins organized in two ports: pins 6, 7, and 8 to be connected to a potentiometer for velocity, and pins 12, 13, 14, and 15 to set the direction (forward or backward). In this way, a two-position joystick is used to control the direction of motor rotation and a potentiometer to adjust the speed. In order to determine the speed profile of the robot, a train of positive and negative steps is set up out of the dead-zone of the motor.

Due to the friction force between components of the same shaft and between the output gears of the same shaft, a minimum intensity of electromotive force is needed to overcome these forces and cause a rotation, so it establishes a minimum voltage level for the coils so that the robot can move forward and overcome this minimum electromotive force. This phenomenon is traditionally called "Dead-Zone" and is found in all motorized elements. In order to characterize this phenomenon, a ramped input is provided, observing the behavior of the output to determine the limits of the dead-zone of the motor. The result of this test is shown in Fig. 15, where the output is given by the estimated velocity of the robot from the motor encoder.

Under the given circumstances, it is exposed to an equivalent voltage ranging between -22.9 V and 23.1 V. The result is a dead zone between -1.73 and 1.5 V.

Now, in order to characterize the dynamic behavior of the motor out of its dead-zone, a train of steps is applied to the motor input, and pulses provided by the encoder are multiplied by the transmission ratio of the motor to obtain the estimated velocity of the robot, giving the response profile obtained in Fig. 16. In order to minimize the effect of the localized noise in the encoder itself, a low-pass filter with a time constant of 100 seconds is applied [5].

As can be seen, the robot responded perfectly to a change of input to the robot, validating the correct operation of both the motor and the encoder, providing the opportunity for future work to be carried out, and implementing different control techniques.

5.1.2. Steering motor

In the case of the steering motor, the same test is repeated both for the dead zone and the saturation limits and to validate the correct operation of the robot. Fig. 17 shows the result of the test for the dead zone, and Fig. 18 shows the angular velocity measured with the encoder with the same filter and orientation of the robot calculated integrating from this velocity [17].

As can be seen, the steering motor has a range of (-23.5 and -0.89) V in the reverse direction and (1.11 and 23.4) V in the clockwise direction. The tests validate the correct functioning of the robot steering.

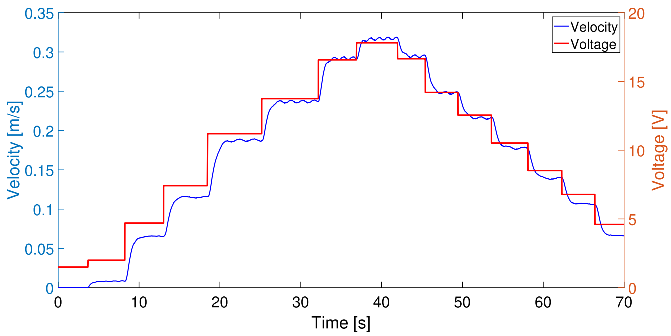

Fig. 16. Raw data from forward open loop test of traction motor.

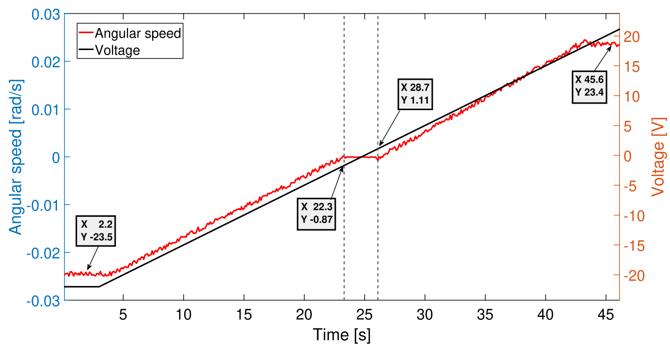

Fig. 17. Dead-Zone response and limited saturation response of steering motor.

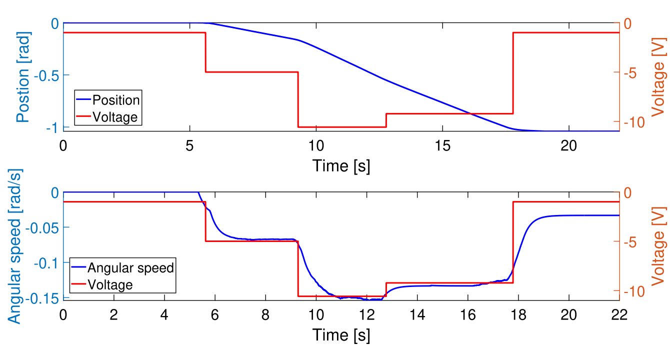

Fig. 18. Raw data from clockwise direction open loop test of steering motor.

These results lay the foundations for future implementation of low-level control algorithms, from Proportional, Integrative, and Derivative (PID) controllers [13], to advanced control techniques, providing the opportunity to implement them in robot simulators [9] for later implementation in the real robot.

5.1.3. Validation of the manoeuvrability of the robot

The main skill that the robot must have is the navigation in the greenhouse. For this, it must be verified that the prototype can navigate through the greenhouse with a load of 100 kg at 0.5 m/s. With the weight well distributed and secured, the robot is manually guided into a greenhouse corridor, providing maximum tension and directly measuring the speed by the encoder. When it reaches the aisle transfer point, the robot turns to the next aisle, thus validating that the prototype can navigate through an aisle in a straight line without problems and that it can turn around with its maximum turning radius. The operator guided this test using the control panel, storing the trajectory in Fig. 19b, with an average speed estimated from the odometry in Fig. 19a.

As observed, the robot can follow a typical zigzag trajectory inside a Mediterranean greenhouse, fulfilling the design specifications. Fig. 20 shows an image of the real robot inside the greenhouse, moving from aisle to aisle and verifying its manoeuvrability.

5.2. Perception subsystems validation

In this section, the sensors performance is evaluated when the robot works alongside operators, analyzing and interpreting their suitability for enabling autonomous navigation. The robot uses the ROS [42] to manage the information provided by the sensors. In particular, it uses ROS 2. ROS represents a set of software libraries and tools designed to facilitate the development of robot applications. From drivers to cutting-edge algorithms and with powerful developer tools, ROS provides everything you need for the development of a robotics project [43]. In addition, all software is available as open source [45]. The Mobile Robot Programming Toolkit (MRPT) library [8] was installed to manage the data from most of the sensors. In addition, the OpenCV 4.2.0 vision library [10] was also used for vision-related tasks and algorithms that focus on SLAM.

Specifically, for Velodyne VLP16 `mola_lidar_odometry` from the MOLA framework [7] was employed, `ORB_SLAM3` to SLAM for Bumblebee [49], the library `MoveNet` that has been developed in [36] for Persee +, and the application provided by the Valeo company `uls_link` for ultrasonic Valeo. The origin is defined at the `base_link` (positioned in the middle of the robot's rear axle), from which the other sensor poses are defined.

- Stereo and RGBD camera: x = right, y = down, z = forward.
- LIDAR: x = forward, y = left, z = up.
- Ultrasonic: Each sensor is reference in `base_link`.

Fig. 21 shows the perception subsystem, equipped with a Bumblebee stereo camera, Velodyne VLP16 3D LiDAR, Orbbec Persee +, and Valeo ultrasonic, with the corresponding reference systems.

These sensors are connected using the diagram in Fig. 22, which details the software connection in ROS and the purpose of each one for the tests carried out in the real greenhouse.

5.2.1. Obstacles map from the ultrasonic sensors

Ultrasounds were installed on the prototype and tested using the tools provided by the provider, Valeo. In this case, the SDKs are provided on a USB stick to work on ROS Noetic or ROS 2 Foxy, together with an application called *uls_link*. This application can be installed on both Linux and Windows, providing the opportunity to perform the first tests efficiently. The calibration is done in the application itself, starting a guided process that calibrates each ultrasound's maximum and minimum ranges.

To validate the installation of these sensors, the robot was placed in front of the operator, standing between the aisles of the greenhouse, and the farmer slowly approaching the front sensors. The result of the test is shown in Fig. 23.

As can be seen, the robot's ultrasounds identify obstacles at the sides due to the tomato row plants themselves and at the front due to the farmer. In this case, when approaching slowly, the obstacle map was checked and the distance designed in Fig. 7 was validated, determining the magnificent behavior of the sensor.

5.2.2. SLAM with Bumblebee

`ORB_SLAM3` is the first real-time SLAM library able to perform Visual, Visual-Inertial, and Multi-Map SLAM with monocular, stereo, and RGB-D cameras, using pinhole and fisheye lens models. In all sensor configurations, `ORB_SLAM3` is as robust as the best systems available in the literature and significantly more accurate [12]. The correct validation of the functioning of the cameras plays a fundamental role in collaborative robotics with humans and cooperative robotics with other robots as it provides the robot with essential characteristics for navigation and joint work. In addition, the large number of objects and the movement

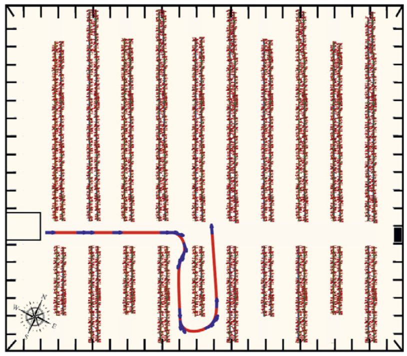

(a) Path travelled between two corridors

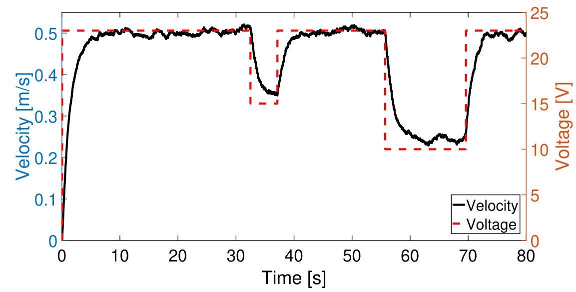

(b) Speed during the path travelled between two corridors

Fig. 19. Validation of the manoeuvrability of the robot.

Fig. 20. AGRICOBIOT II making a turn in the shuttle between corridors in the greenhouse.

Fig. 21. Perception subsystem mounted on the robot. The x-axis is represented in red, the y-axis in green, and the z-axis in blue.

of operators within a greenhouse make it difficult to use traditional algorithms in ideal environments, which is a unique challenge today. For this reason, this article shows the design of a robot with sensors installed for immediate use of the most commonly used technologies, validating their correct functioning for future autonomous navigation. In this case, the robot aims to identify the farmer in the tasks to be carried out, ensuring collaboration and interaction between the human and the machine.

- **Bumblebee calibration**

The intrinsic parameters of the stereo camera were determined using the `kinect-stereo-calib` application from the Mobile Robot Programming Toolkit (MRPT) [8]. These parameters include the focal lengths (f_x, f_y), optical centers (c_x, c_y), pin-hole distortion parameters (k_1, k_2, p_1, p_2), and the left-to-right relative pose. Extrinsic parameters specify the relative poses of different sensor frames of reference. In this case, the same method has been followed as in [15] since it is the same camera for the same purpose.

- **SLAM Bumblebee test**

The test was carried out by placing the robot next to the farmer as he picked fruit at different heights in the crop during the harvesting season. The stereo camera has two lenses (Fig. 24a and 24b) showing how the operator performs a harvesting task. The results are shown in Fig. 25.

It can be seen how the mapping has identified the operator, validating the correct functioning of the camera intended for obstacle detection in navigation.

5.2.3. SLAM with Velodyne VLP16

With the same test performed with the camera, the robot design will be validated with the Velodyne VLP16. The LiDAR was calibrated according to [28], guaranteeing the quality of the data. The human moves slightly forward, and the robot observes him, obtaining a point cloud in real time. The result of the mapping obtained is shown in Fig. 26a, showing a frame obtained from the recorded data set [14].

- **LiDAR calibration**

To perform the Velodyne VLP16 LiDAR calibration, the steps described in [30] were followed, optimizing the error in the Euclidean distance of 50 manually selected correspondences and a robust measure on the disparity error with respect to the three top performing stereo methods in the KITTI stereo benchmark [29].

- **SLAM LiDAR test**

Figs. 26a and 26b show the result of performing SLAM with MOLA while the farmer performs the harvesting task.

In addition, the mapping identifies the surrounding plants, allowing navigation through the greenhouse [15]. Furthermore, there is a clear difference between a greenhouse corridor with and without a farmer. In this case, it can be seen how the LiDAR perfectly captures the farmer, allowing the implementation of collaborative strategies in the future.

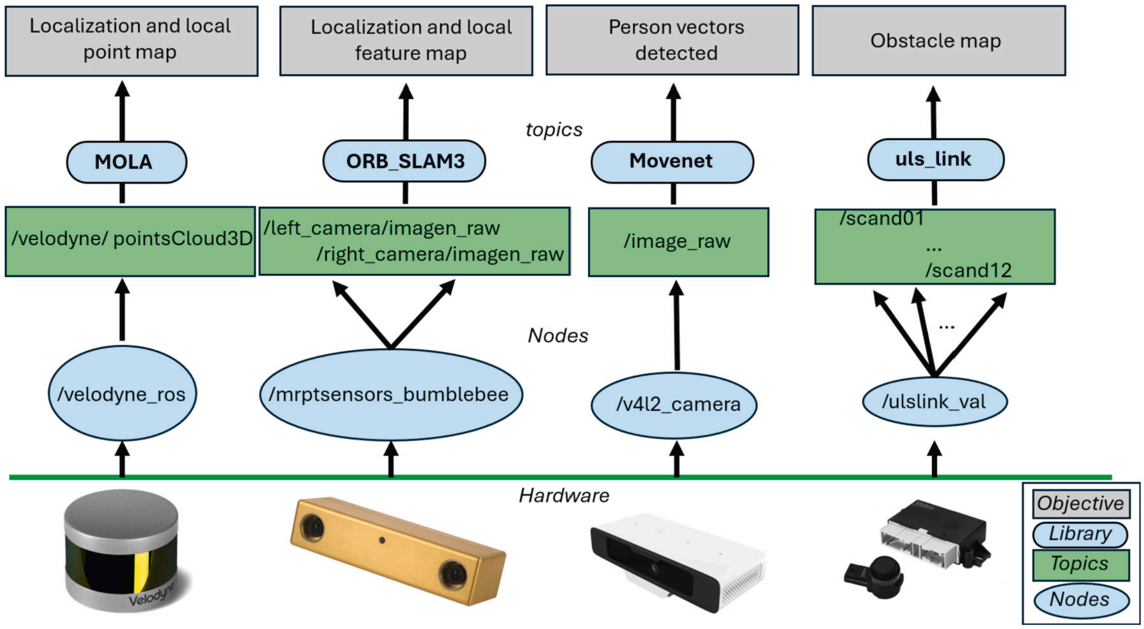

Fig. 22. ROS connection diagram.

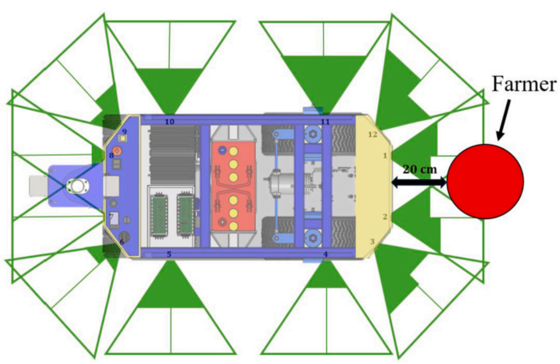

Fig. 23. Valeo obstacle map test.

5.2.4. Pose detection with Orbbec Persee +

The `MoveNet` library is designed to process raw camera images and convert them into valuable inputs for vision algorithms: rectified mono/color images, stereo disparity images, and stereo point clouds. In this case, on the basis of [25], where the authors use a binocular camera, it is possible to determine the pose of a human. This library can be installed on the camera's own Ubuntu 18.04 operating system, allowing it to work on its own and freeing the main computer from the burden of image reconstruction. As was previously commented, in the greenhouse scenario, farmer recognition is fundamental in establishing correct communication between humans and robots. Therefore, along the same lines as the previous validations, the same test will be carried out to ensure correct operation.

- **Presee + calibration**

For the calibration of this camera, the library itself provides a tool called `camera calibration` that calibrates monocular and stereo cameras in the ROS system. The Camera Info page provides a detailed description of the parameters used by the `Movenet`.

- **Pose detection Persee + test**

Repeating the same experiment, Fig. 27 shows the result of farmer identification.

In this case, we can see how it draws an image perfectly positioned with the operator, providing an excellent opportunity to implement more advanced collaborative robotics algorithms in the future.

6. Conclusions

This paper presents the development of a novel *Ackermann*-type collaborative mobile agricultural robot to provide transport work inside greenhouses together with farmers. Furthermore, the robot is equipped with enough technology to establish an internet connection, thus entering the new era of Industry 4.0 with the Internet of Things (IoT) and laying the first foundations for cooperation with other agricultural machinery. The article explains the process from the first idea-driven brush strokes to validating all mobile robotics sensors for collaborating next to the operator. The results meet the expectations of the development itself, as well as being able to perform tests on the prototype with real farmers in the area. Continuous improvement of this type of agricultural robot is crucial to promote research in such a complicated environment as a greenhouse, specially in Mediterranean greenhouses, where there is still much to be perfected.

At present, there is no prototype capable of carrying such a large payload through the greenhouse and of navigating in such a complex environment without being a problem for the environment. This design allows the community of researchers to test the most commonly used algorithms to perform tasks such as SLAM, people detection, obstacle mapping, etc., in a unique agricultural environment focused on intensive agriculture under greenhouses. Mapping, orientation, and precise navigation are crucial for various robotic activities within greenhouses, particularly on the transport task.

This novel design is intended to usher in a new generation of agricultural robots, laying the mechanical foundations for moving smoothly through a typical Mediterranean greenhouse and the foundations for the hardware needed to make collaborative journeys with agriculture at the height of the vegetable harvesting season. However, this prototype will continue to improve as this article is only the first step to being able to carry out various tasks inside the greenhouse, from the systematic comparison of the autonomous navigation of this *Ackermann* robot and a differential robot working cooperatively to the monitoring of the state of the crop, growth or pest detection thanks to the sensors installed and validated in this work.

(a) Left raw image (b) Right raw image

Fig. 24. Stereo image of Bumblebee.

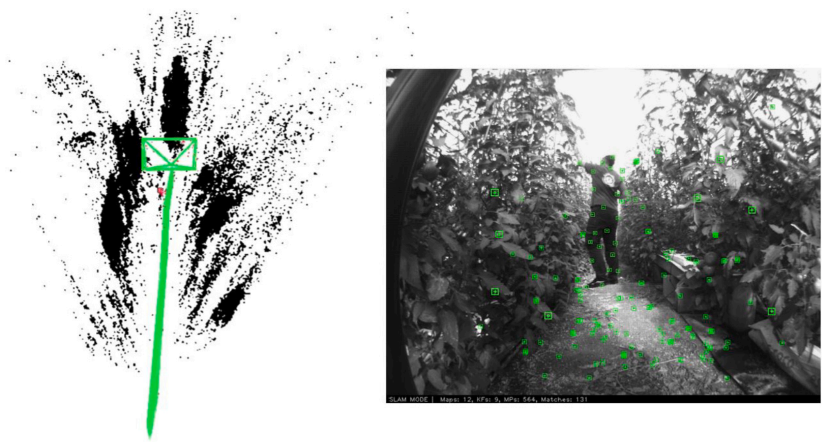

Fig. 25. SLAM of Bumblebee next to farmer with `ORB-SLAM3`.

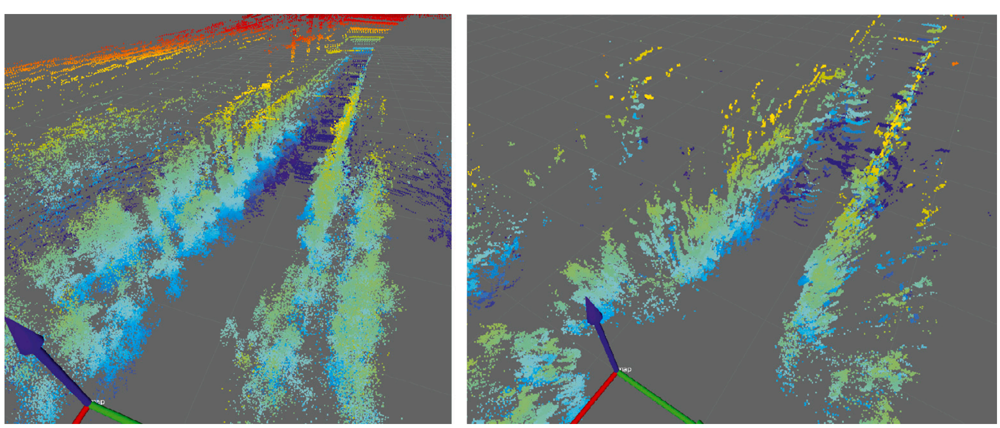

(a) SLAM of Velodyne VLP16 without farmer (b) SLAM of Velodyne VLP16 next to farmer

Fig. 26. SLAM Velodyne test with a jet type color intensity.

The next step will be the implementation in ROS 2 Humble of different control techniques that allow us to trace and determine the speed and direction of the robot itself between a displacement between an origin and an end. Currently, the robot has the necessary technology to establish a closed loop by implementing different control techniques, from the odometry captured by the encoders to navigation algorithms based on the orientation provided by the LiDAR sensors or stereo cameras. In addition, the vision system provides the opportunity to implement pest identification algorithms, adaptation to different types of terrain, and mathematical models of plant growth, among others.

This paper aims to present and share the development of how to implement an agricultural robot in a complicated environment. As already mentioned, some robots navigate inside greenhouses. However, they need to have the capacity to carry a large payload, establish collaborative work with humans, and have the basic technology to connect to the internet to manage and monitor the different variables of the environment. The validation of all the sensors provides solid support to the most important objectives of this project, offering an apparent reference for researchers to use as a starting point for improving their agricultural machines and navigation algorithms.

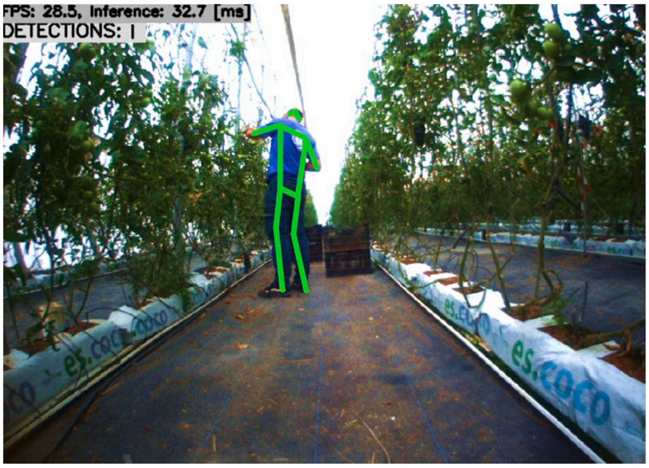

Fig. 27. Pose detection farmer inside greenhouse.

CRediT authorship contribution statement

Fernando Cañadas-Aránega: Writing – review & editing, Writing – original draft, Visualization, Validation, Supervision, Software, Resources, Methodology, Investigation, Formal analysis, Data curation, Conceptualization. **José C. Moreno:** Writing – review & editing, Visualization, Validation, Project administration, Methodology, Investigation, Funding acquisition, Formal analysis, Conceptualization. **José L. Blanco-Claraco:** Writing – review & editing, Visualization, Validation, Software, Methodology, Investigation, Formal analysis, Data curation, Conceptualization. **Antonio Giménez:** Project administration, Methodology, Investigation, Funding acquisition, Conceptualization. **Francisco Rodríguez:** Writing – review & editing, Methodology, Investigation, Formal analysis, Conceptualization. **Julián Sánchez-Hermosilla:** Writing – review & editing, Conceptualization.

Declaration of competing interest

The authors declare that they have no known competing financial interests or personal relationships that could have appeared to influence the work reported in this paper.

Acknowledgements

This work has been partially financed by the 'CyberGreen' Project, PID2021-122560OB-I00, and the 'AgroConnect.es' infrastructure used to carry out this research, grant EQC2019-006658-P, both funded by MCIN/AEI/ 10.13039/501100011033 and by FEDER A way to make Europe. Also, author Fernando Cañadas-Aránega is supported by an FPI (PRE2022-102415) grant from Spanish Ministry of Science, Innovation and Universities.

Data availability

No data was used for the research described in the article.

References

[1] A. Abanay, L. Masmoudi, M. El Ansari, J. Gonzalez-Jimenez, F.A. Moreno, Lidar-based autonomous navigation method for an agricultural mobile robot in strawberry greenhouse: Agrieco robot, AIMS Electron. Electr. Eng. 6 (2022) 317–328.
[2] AENOR, Ea 95 steel profiles, NBA EA 95, https://lim.ii.udc.es/docencia/din-sismec/perfiles_ea_95.pdf, 2011.
[3] A.S. Aguiar, F.N. dos Santos, J.B. Cunha, H. Sobreira, A.J. Sousa, Localization and mapping for robots in agriculture and forestry: a survey, Robotics 9 (2020) 97.
[4] V. Ahumada-Newhart, J.S. Olson, Going to school on a robot: robot and user interface design features that matter, ACM Trans. Comput.-Hum. Interact. (TOCHI) 26 (2019) 1–28.
[5] K.J. Åström, R.M. Murray, Feedback Systems: An Introduction for Scientists and Engineers, Princeton University Press, 2021.
[6] C. Bac, J. Hemming, E. Van Henten, Robust pixel-based classification of obstacles for robotic harvesting of sweet-pepper, Comput. Electron. Agric. 96 (2013) 148–162.
[7] J.L. Blanco-Claraco, A modular optimization framework for localization and mapping, in: Robotics: Science and Systems, Freiburg im Breisgau, Germany, 2019, pp. 1–15.
[8] J.L. Blanco-Claraco, N. Koukis, H. Laux, N. Alice, J. Briales, J. Monroy, jotaraul, M.J. Tarifa, R. Sahdev, E. Fernandez-Moral, F. Moreno, miguelcastillon, M.L. Antequera, A. Partow, G. Yengera, M. Bellone, David, emilkhatib, P. Rudolph, Y. Ochiai, S. Talbert, N. Demmel, Logrus, J.S. Simón, L.D. Más, O. Adiyatov, R. Voorhies, T. Shen, alibenD, Mrpt/mrpt: Release of v2.11.7, https://doi.org/10.5281/zenodo.10595287, 2024.
[9] J.L. Blanco-Claraco, B. Tymchenko, F.J. Mañas-Alvarez, F. Cañadas-Aránega, Á. López-Gázquez, J.C. Moreno, Multivehicle simulator (mvsim): lightweight dynamics simulator for multiagents and mobile robotics research, SoftwareX 23 (2023) 101443.
[10] G. Bradski, A. Kaehler, Learning OpenCV: Computer Vision with the OpenCV Library, O'Reilly Media, Inc., 2008.
[11] I.E. Britannica, Encyclopaedia. Nabu Press, 2022.
[12] C. Campos, R. Elvira, J.J. Gómez, J.M.M. Montiel, J.D. Tardós, ORB-SLAM3: an accurate open-source library for visual, visual-inertial and multi-map SLAM, IEEE Trans. Robot. 37 (2021) 1874–1890.
[13] F. Cañadas-Aránega, J.C. Moreno, J.L. Blanco-Claraco, A pid-based control architecture for mobile robot path planning in greenhouses, IFAC-PapersOnLine 58 (2024) 503–508.
[14] F. Cañadas-Aránega, Rawlog pointcloud of the agricobiot ii robot working next to farmer, https://youtu.be/eQWtcuyJQFU, 2024.
[15] F. Cañadas-Aránega, J.L. Blanco-Claraco, J.C. Moreno, F. Rodriguez-Diaz, Multimodal mobile robotic dataset for a typical Mediterranean greenhouse: the greenbot dataset, Sensors 24 (2024), https://doi.org/10.3390/s24061874, https://www.mdpi.com/1424-8220/24/6/1874.
[16] A. Choudhary, Y. Kobayashi, F.J. Arjonilla, S. Nagasaka, M. Koike, Evaluation of mapping and path planning for non-holonomic mobile robot navigation in narrow pathway for agricultural application, in: 2021 IEEE/SICE International Symposium on System Integration (SII), IEEE, 2021, pp. 17–22.
[17] P.I. Corke, O. Khatib, Robotics, Vision and Control: Fundamental Algorithms in MATLAB, vol. 73, Springer, 2011.
[18] J. Crespo, R. Barber, O. Mozos, Relational model for robotic semantic navigation in indoor environments, J. Intell. Robot. Syst. 86 (2017) 617–639.
[19] A. Durmanov, N. Saidaxmedova, M. Mamatkulov, K. Rakhimova, N. Askarov, S. Khamrayeva, A. Mukhtorov, S. Khodjimukhamedova, T. Madumarov, K. Kurbanova, Emerging science journal sustainable growth of greenhouses: investigating key enablers and impacts, Emerg. Sci. J. 7 (2023) 2610–9182, https://doi.org/10.28991/ESJ-2023-07-05-014, www.ijournalse.org.
[20] P.O. Dusadeerungsikul, S.Y. Nof, A collaborative control protocol for agricultural robot routing with online adaptation, Comput. Ind. Eng. 135 (2019) 456–466.
[21] R.A. Epstein, E.Z. Patai, J.B. Julian, H.J. Spiers, The cognitive map in humans: spatial navigation and beyond, Nat. Neurosci. 20 (2017) 1504–1513.
[22] G.G. Etxebarria, Agencia Europea para la seguridad y la salud en el trabajo (EU-OSHa). Reglamento (UE) 2019/126 del Parlamento Europeo y del Consejo de 16 de enero de 2019. Gestión práctica de riesgos laborales: Integración y desarrollo de la gestión de la prevención, 2019, pp. 56–72.
[23] M. Fairbairn, J. Guthman, Agri-food tech discovers silver linings in the pandemic, Agric. Human Values 37 (2020) 587–588.
[24] FAO, How to Feed the World in 2050. URL, https://www.fao.org/fileadmin/templates/wsfs/docs/expert_paper/How_to_Feed_the_World_in_2050.pdf, 2024.
[25] W. Feng, Z. Liang, J. Mei, S. Yang, B. Liang, X. Zhong, J. Xu, Petroleum pipeline interface recognition and pose detection based on binocular stereo vision, Processes 10 (2022) 1722.
[26] Z. Feng, G. Hu, Y. Sun, J. Soon, An overview of collaborative robotic manipulation in multi-robot systems, Annu. Rev. Control 49 (2020) 113–127.
[27] D.L. Gabriel, J. Meyer, F. Du Plessis, Brushless dc motor characterisation and selection for a fixed wing uav, in: IEEE Africon'11, 2011, pp. 1–6.
[28] A. Geiger, P. Lenz, C. Stiller, R. Urtasun, Vision meets robotics: the kitti dataset, Int. J. Robot. Res. 32 (2013) 1231–1237.
[29] A. Geiger, P. Lenz, R. Urtasun, Are we ready for autonomous driving? The kitti vision benchmark suite, in: 2012 IEEE Conference on Computer Vision and Pattern Recognition, IEEE, 2012, pp. 3354–3361.
[30] A. Geiger, F. Moosmann, O. Car, B. Schuster, A toolbox for automatic calibration of range and camera sensors using a single shot, in: Proceedings of International Conference on Robotics, 2012, and Automation (ICRA).
[31] B. Gogoi, T. Nath, D. Kashyap, S. Sarma, R. Kalita, Chapter 15 - sustainable agriculture, forestry and fishery for bioeconomy, Elsevier, 2020, https://www.sciencedirect.com/science/article/pii/B9780444643094000155, https://doi.org/10.1016/B978-0-444-64309-4.00015-5.
[32] K. Goris, Autonomous mobile robot mechanical design, VrijeUniversiteitBrussel, Engineering Degree Thesis, 2005, Brussels, Belgium.
[33] J. Hernández, S. Bonachela, M.R. Granados, J.C. López, J.J. Magán, J.I. Montero, Microclimate and agronomical effects of internal impermeable screens in an unheated Mediterranean greenhouse, Biosyst. Eng. 163 (2017) 66–77.

[34] G. Hick, World greenhouse vegetable statistics- 2019 updates cuesta roble greenhouse vegetable consulting, Agric. Human Values (2019).
[35] R. Irani, R. Bauer, A. Warkentin, A dynamic terramechanic model for small lightweight vehicles with rigid wheels and grousers operating in sandy soil, J. Terramech. 48 (2011) 307–318.
[36] B. Jo, S. Kim, Comparative analysis of openpose, posenet, and movenet models for pose estimation in mobile devices, Trait. Signal 39 (2022) 119.
[37] R. Kelly, Robust asymptotically stable visual servoing of planar robots, IEEE Trans. Robot. Autom. 12 (1996) 759–766.
[38] N. Khan, R.L. Ray, G.R. Sargani, M. Ihtisham, M. Khayyam, S. Ismail, Current progress and future prospects of agriculture technology: gateway to sustainable agriculture, Sustainability 13 (2021) 4883.
[39] M.H. Ko, B.S. Ryuh, K.C. Kim, A. Suprem, N.P. Mahalik, Autonomous greenhouse mobile robot driving strategies from system integration perspective: review and application, IEEE/ASME Trans. Mechatron. 20 (2014) 1705–1716.
[40] R.G. Lins, S.N. Givigi, Cooperative robotics and machine learning for smart manufacturing: platform design and trends within the context of industrial Internet of things, IEEE Access 9 (2021) 95444–95455.
[41] C. Lytridis, V.G. Kaburlasos, T. Pachidis, M. Manios, E. Vrochidou, T. Kalampokas, S. Chatzistamatis, An overview of cooperative robotics in agriculture, Agronomy 11 (2021) 1818.
[42] S. Macenski, T. Foote, B. Gerkey, C. Lalancette, W. Woodall, Robot operating system 2: design, architecture, and uses in the wild, Sci. Robot. 7 (2022) eabm6074.
[43] S. Macenski, T. Foote, B. Gerkey, C. Lalancette, W. Woodall, Robot operating system 2: design, architecture, and uses in the wild, Sci. Robot. 7 (2022) eabm6074, https://doi.org/10.1126/scirobotics.abm6074, https://www.science.org/doi/abs/10.1126/scirobotics.abm6074.
[44] A. Mandow, J. Gomez-de Gabriel, J.L. Martinez, V.F. Munoz, A. Ollero, A. Garcia-Cerezo, The autonomous mobile robot aurora for greenhouse operation, IEEE Robot. Autom. Mag. 3 (1996) 18–28.
[45] W. Meeussen, M. Wise, S. Glaser, S. Chitta, C. McGann, P. Mihelich, E. Marder-Eppstein, M. Muja, V. Eruhimov, T. Foote, et al., Autonomous door opening and plugging in with a personal robot, in: 2010 IEEE International Conference on Robotics and Automation, IEEE, 2010, pp. 729–736.
[46] L.E. Montoya-Cavero, R.D. de León Torres, A. Gómez-Espinosa, J.A.E. Cabello, Vision systems for harvesting robots: produce detection and localization, Comput. Electron. Agric. 192 (2022) 106562.
[47] J.C. Moreno Úbeda, F. Cañadas-Aránega, F. Rodríguez, J. Sánchez-Hermosilla, A. Giménez, Modelado 3d y diseño de un robot colaborativo para tareas de transporte en invernaderos, in: XLIII Jornadas de Automática, Universidade da Coruña. Servizo de Publicacións, 2022, pp. 785–791.
[48] H. Mousazadeh, A technical review on navigation systems of agricultural autonomous off-road vehicles, J. Terramech. 50 (2013) 211–232.
[49] R. Mur-Artal, J.D. Tardós, ORB-SLAM2: an open-source SLAM system for monocular, stereo and RGB-D cameras, IEEE Trans. Robot. 33 (2017) 1255–1262, https://doi.org/10.1109/TRO.2017.2705103.
[50] M. Muñoz, J.L. Guzmán, J.A. Sánchez-Molina, F. Rodríguez, M. Torres, M. Berenguel, A new iot-based platform for greenhouse crop production, IEEE Int. Things J. 9 (2022) 6325–6334, https://doi.org/10.1109/JIOT.2020.2996081.
[51] K. Nemali, History of controlled environment horticulture: greenhouses, HortScience 57 (2022) 239–246, https://doi.org/10.21273/HORTSCI16160-21, https://journals.ashs.org/hortsci/view/journals/hortsci/57/2/article-p239.xml.
[52] A. Popescu, M.I. Nazare, D. Olaru, Friction torque in a modified angular contact ball bearing operating at low axial loads, IOP Conf. Ser., Mater. Sci. Eng. 444 (2018) 022019.
[53] V. Rijswick, World vegetable map 2018. Global trade still fruitful, Technical report. RaboResearch Food & Agribussiness https://research.rabobank.com/far/en/sectors/regional-food-agri/world_fruit_map_2018.html, 2018.
[54] C.D.P. Rodrigues, Design of a High-Speed Transmission for an Electric Vehicle, 2018.
[55] F. Rodríguez, J. Moreno, J. Sánchez, M. Berenguel, Grasping in agriculture: state-of-the-art and main characteristics, in: Grasping in Robotics, 2013, pp. 385–409.
[56] J. Sánchez-Hermosilla, R. González, F. Rodríguez, J. Donaire, Mechatronic description of a laser autoguided vehicle for greenhouse operations, Sensors 13 (2013) 769–784, https://doi.org/10.3390/s130100769, http://www.ncbi.nlm.nih.gov/pubmed/23299624, http://www.pubmedcentral.nih.gov/articlerender.fcgi?artid=PMC3574703, http://www.mdpi.com/1424-8220/13/1/769.
[57] J. Sanchez-Hermosilla, F. Rodriguez, R. Gonzalez, J.L. Guzman, M. Berenguel, A mechatronic description of an autonomous mobile robot for agricultural tasks in greenhouses, in: A. Barrera (Ed.), Mobile Robots Navigation, IntechOpen, Rijeka, 2010, chapter 29.
[58] J. Sánchez-Molina, F. Rodríguez, J. Moreno, J. Sánchez-Hermosilla, A. Giménez, Robotics in greenhouses. scoping review, Comput. Electron. Agric. 219 (2024) 108750.
[59] SKF, Catálogo General de Rodamientos, 2015, SKF, Argentina. PUBBUU/P1 100000/A ES.
[60] D.S. SolidWorks, Solidworks®. Version Solidworks 1, 2005.
[61] J. Spijker, J. Pérez Díaz, A.D. Cámara Hueso, 2008, Generational changes in stature in 20th century Spain from the National Health Survey.
[62] H. Tian, T. Wang, Y. Liu, X. Qiao, Y. Li, Computer vision technology in agricultural automation—a review, Inf. Process. Agric. 7 (2020) 1–19.
[63] F. Vicentini, Collaborative robotics: a survey, J. Mech. Des. 143 (2021) 040802.
[64] D. Xie, L. Chen, L. Liu, L. Chen, H. Wang, Actuators and sensors for application in agricultural robots: a review, Machines 10 (2022) 913.
[65] Y. Zhao, L. Gong, Y. Huang, C. Liu, A review of key techniques of vision-based control for harvesting robot, Comput. Electron. Agric. 127 (2016) 311–323.
[66] H. Zhong, S.Y. Nof, S. Berman, Asynchronous cooperation requirement planning with reconfigurable end-effectors, Robot. Comput.-Integr. Manuf. 34 (2015) 95–104.
[67] H. Zhong, J.P. Wachs, S.Y. Nof, A collaborative telerobotics network framework with hand gesture interface and conflict prevention, Int. J. Prod. Res. 51 (2013) 4443–4463.